Evolution of Technetium Speciation in Reducing Grout

Wayne W. Lukens, Jerome J. Bucher, David K. Shuh, and Norman M. Edelstein*

Actinide Chemistry Group

Chemical Sciences Division

Lawrence Berkeley National Laboratory

Berkeley, CA 94720

wwlukens@lbl.gov, phone: (510) 486-4305, FAX: (510) 486-5596

RECEIVED DATE (to be automatically inserted after your manuscript is accepted if required according to the journal that you are submitting your paper to)

ABSTRACT Cementitious waste forms (CWFs) are an important component of the strategy to stabilize high-level nuclear waste resulting from plutonium production by the U.S. Department of Energy (DOE). Technetium (^{99}Tc) is an abundant fission product of particular concern in CWFs because of the high solubility and mobility of Tc(VII), pertechnetate (TcO_4^-) the stable form of technetium in aerobic environments. CWFs can more effectively immobilize ^{99}Tc if they contain additives that reduce mobile TcO_4^- to immobile Tc(IV) species. The ^{99}Tc leach rate of reducing CWFs that contain Tc(IV) is much lower than for CWFs that contain TcO_4^-. Previous X-ray absorption fine structure (XAFS) studies showed that Tc(IV) species were oxidized to TcO_4^- in reducing grout samples prepared on a laboratory scale. Whether the oxidizer was atmospheric O_2 or NO_3^- in the waste simulant was not determined. In actual CWFs, rapid oxidation of Tc(IV) by NO_3^- would be of concern, whereas oxidation by atmospheric O_2 would be of less concern due to the slow diffusion and reaction of O_2 with the reducing CWF. To address this uncertainty, two series of reducing grouts were prepared using TcO_4^- containing

waste simulants with and without NO_3^-. In the first series of samples, referred to as "permeable samples", the TcO_4^- was completely reduced using Na_2S, and the samples were sealed in cuvettes made of polystyrene, which has a relatively large O_2 diffusion coefficient. In these samples, all of the technetium was initially present as a Tc(IV) sulfide compound, TcS_x, which was characterized by extended X-ray absorption fine structure (EXAFS) spectroscopy. The EXAFS data is consistent with a structure consisting of triangular clusters of Tc(IV) centers linked together through a combination of disulfide and sulfide bridges as in MoS_3. From the EXAFS model, the stoichiometry of TcS_x is Tc_3S_{10}, and TcS_x is presumably the compound generally referred to as Tc_2S_7. The TcS_x initially present in the permeable samples was steadily oxidized over 4 years. In the second series of samples, called "impermeable samples", the TcO_4^- was not completely reduced initially, and the grout samples were sealed in cuvettes made of poly(methyl methacrylate), which has a small O_2 diffusion coefficient. In the impermeable samples, the remaining TcO_4^- continued to be reduced, presumably by blast furnace slag in the grout, as the samples aged. When the impermeable samples were opened and exposed to atmosphere, the lower-valent technetium species were rapidly oxidized to TcO_4^-.

MANUSCRIPT TEXT

Introduction Remediation of the sites used by the U. S. Department of Energy (DOE) for plutonium production is one of the most expensive and complex remediation projects in the U. S.[1,2] An important component of this effort is the use of grout based cementitious waste forms (CWFs) at the Savannah River Site to solidify and stabilize the low-activity waste stream and to stabilize the waste residues in high-level tanks.[3-6] The long-term effectiveness of these measures to prevent the migration of radionuclides is described by performance assessments that depend on the leach rates of the radionuclides.[3,5,7,8] ^{99}Tc is one of the radionuclides of greatest concern for leaching from CWFs because of the high mobility and lack of sorption of Tc(VII), pertechnetate (TcO_4^-), the most stable form of technetium under aerobic conditions.[8,9]

For soluble contaminants such as TcO_4^- or NO_3^-, leach rates from CWFs can be modeled using an effective diffusion coefficient, $D_{eff} = D_m/N_m$, where D_m is the molar diffusion coefficient of the contaminant in water and N_m is the MacMullin number, a characteristic of the porous solid that is identical for solutes such as gases or anions that are highly soluble and not adsorbed by the matrix.[10,11] Among potential CWFs, the effective diffusion coefficient of nitrate, $D_{eff(NO3-)}$, varies from 1.3×10^{-9} cm^2 s^{-1} to 6.2×10^{-8} cm^2 s^{-1}.[5,9,12] The D_{eff} values for NO_3^- and TcO_4^- are similar since their molar diffusion coefficients are almost identical: 1.53×10^{-5} cm^2 s^{-1} and 1.48×10^{-5} cm^2 s^{-1}, respectively.[13,14] The leachability of technetium can be greatly decreased by reducing soluble TcO_4^- to relatively insoluble Tc(IV) by the addition of blast furnace slag (BFS) or other reductants to the grout. The $D_{eff(99Tc)}$ values of reducing grouts are much smaller than in ordinary CWFs, 3×10^{-11} cm^2 s^{-1} to 4×10^{-12} cm^2 s^{-1}, because Tc(IV) has low solubility and is readily adsorbed by the grout matrix.[9,12] Reducing conditions are used in actual CWFs to take advantage of this decreased leachability and create a more effective waste form.[6,12]

A previous research study showed that although TcO_4^- is reduced to Tc(IV) in reducing grouts, the degree of reduction varied with experimental conditions.[15] In some cases, TcO_4^- was initially reduced to Tc(IV) but was later oxidized. Two species, NO_3^- and O_2, are present in large quantities in or around CWFs and are potentially capable of oxidizing Tc(IV) to TcO_4^-. Whether NO_3^- or O_2 is responsible for oxidizing Tc(IV) has a profound effect on the behavior of technetium in CWFs. If NO_3^- is chiefly responsible for the oxidation, Tc(IV) would be oxidized throughout the entire CWF, increasing the leachability of ^{99}Tc in the entire volume of the waste. In this scenario, the rate of oxidation of Tc(IV) to TcO_4^- would depend only on the reaction rate and the concentration of the reactants.

The scenario involving oxidation by O_2 is more complicated. In this case, diffusion of O_2 into the CWF would result in the formation of an oxidized surface region in the grout in contact with oxygenated

surface water. This surface region would have greater technetium leachability that would be similar to that of CWFs that do not contain reducing agents. However, the leachability of technetium in the bulk of the waste would be unchanged since it would remain Tc(IV). As shown by Smith and Walton, the thickness of the oxidized region depends mainly upon the rate of oxygen diffusion and the reductive capacity of the CWF.[16] Using typical parameters for reducing CWFs, the thickness of the oxidized region is small compared to the dimensions of the CWF at times comparable to the half-life of ^{99}Tc, so oxidation by O_2 is of less concern than oxidation by NO_3^-.

Therefore, the primary concern raised by the rapid oxidation of Tc(IV) observed in the previous study was the possibility that NO_3^- rather than O_2 was responsible for the oxidation. Rapid oxidation of Tc(IV) by NO_3^- would mean that all of the initially reduced technetium in actual CWFs would be quickly oxidized back to TcO_4^-. In this paper, the evolution of ^{99}Tc speciation in a series of grout samples in containers with very different O_2 permeabilities and with and without NO_3^- was followed for an extended period, using X-ray absorption fine structure (XAFS), to determine whether NO_3^- or O_2 was responsible for oxidizing Tc(IV) species in these grout samples.

Experimental Section

Procedures. *Caution: ^{99}Tc is a β-emitter (E_{max} = 294 keV, $\tau_{1/2} = 2 \times 10^5$ years).* All operations were carried out in a radiochemical laboratory equipped for handling this isotope. Technetium, as $NH_4^{99}TcO_4$, was obtained from Oak Ridge National Laboratory and was purified as previously described.[17] Where available, the standard deviation of measured and calculated values are included in parentheses following the value and are in the same units as the last digit.

All operations were carried out in air. Water was deionized, passed through an activated carbon cartridge to remove organic material and then distilled. All other chemicals were used as received. The grout samples are similar to those previously used for the study of chromium reduction in reducing

grout samples and are similar to Saltstone, the CWF used to immobilize low activity waste at the Savannah River Site.[12,18] The dry grout components consisted of 46% Type F fly ash, 46% BFS, and 8% Portland cement.[18] The fly ash, BFS, and Portland cement are those used by the Savannah River Saltstone facility, and were provided by C. A. Langton. Two series of grout samples were prepared and were assumed to have a density of 1.7 g cm^{-3}.[19] The cuvettes were standard semi-micro cuvettes with interior dimensions of 1.0 × 0.4 × 4.5 cm.

The first series of samples was prepared using waste simulants with and without NO_3^- and NO_2^- as shown in Table 1. To the waste simulant was added TcO_4^- (0.02 mmol, 0.1 mL, 0.2 M NH_4TcO_4), which was then reduced with Na_2S (0.29 mmol, 0.1 mL, 2.9 M) in 1 M LiOH forming a very dark solution with a black precipitate. The dry grout components were added forming a slurry that was placed in a polystyrene (PS) cuvette, which was capped and closed with vinyl tape then sealed inside two 0.05 mm polyethylene (PE) bags. This first series of samples will be referred to as "permeable samples" since O_2 has a high diffusion coefficient of 2.3×10^{-7} cm^2 s^{-1} in PS.[20,21] The final composition of the waste solution after addition of the TcO_4^- and Na_2S solutions is listed in Table 1.

The second series of samples was prepared analogously to the first. To the waste simulant was added TcO_4^- (0.012 mmol, 0.30 mL, 0.039 M $NaTcO_4$) and Na_2S (0.05 mmol, 0.065 mL, 0.8 M) in 1 M LiOH (same solution as above, which had oxidized from air exposure), forming a dark solution with a black precipitate. The dry grout components were added, forming a slurry that was placed in a poly-(methyl methacrylate) (PMMA) cuvette that was sealed with a plug of epoxy and further sealed inside two 0.1 mm (PE) bags. This second series of samples will be referred to as "impermeable samples" since O_2 has a very low diffusion coefficient of 2.3×10^{-9} cm^2 s^{-1} in PMMA.[22] The final composition of the waste solution after addition of the TcO_4^- and Na_2S solutions is also listed in Table 1. Samples A and C were opened after 26 months and placed in loosely capped jars that were fully opened weekly. The grout

samples removed from the cuvettes and used for XAFS studies measured 1.0 × 0.4 × ~1.0 cm, and retained the flat surfaces of the cuvette. Sample B remained sealed.

Table 1: Composition of cement samples

Sample	Tc (mg)	Solution (mL)	Final Solution Composition	Dry grout mixture (g)
			Permeable Samples	
1	2	1.5	1.85 M $NaNO_3$, 1.07 M NaOH, 0.57 M $NaNO_2$, 0.23 M $NaAl(OH)_4$, 0.16 M Na_2CO_3, 0.14 M Na_2SO_4, 0.02 M NaCl, 0.02 M $Na_2C_2O_4$, 0.008 M Na_3PO_4, 0.13 M Na_2S	3
2	2	1.5	As Sample 1, but no $NaNO_3$, $NaNO_2$	3
3	2	0.95	As Sample 1, but 0.05 M Na_3PO_4	1.5
4	2	0.95	As Sample 2, but 0.05 M Na_3PO_4	1.5
			Impermeable Samples	
A	1.2	0.66	2 M NaOH, 2 M NaCl	1.0
B	1.2	0.66	2 M NaOH, 2 M $NaNO_3$	1.0
C	1.2	0.66	2 M NaOH, 2 M $NaNO_2$	1.0

The reductive capacity of the BFS was determined using a slightly modified version of the Angus and Glasser method.[23] The BFS (~0.5 g) was slurried in 5-10 mL of water to which was added 25.0 mL of 0.059 M $(NH_4)_4Ce(SO_4)_4 \cdot 2H_2O$ in 2 M sulfuric acid. After 1 hour, the solution was titrated with freshly prepared 0.050 M $(NH_4)_2Fe(SO_4)_2 \cdot 6H_2O$ in 0.75 M sulfuric acid. The end point was determined using 0.25 mL of 0.025 M Fe(II) tris-(1,10-phenanthroline) complex.[24,25] The reductive capacity of the BFS sample was 0.82(1) meq g^{-1} as determined from the difference in the volume of Fe(II) solution needed to titrate 25.0 mL of the Ce(IV) solution alone and with the BFS. Analysis of the sulfide content of

Na_2S in 1 M LiOH, which was used to reduce the TcO_4^- in the grout samples, was performed analogously by comparison with a sample of freshly recrystallized $Na_2S•9H_2O$. Determination of the reductive capacity of BFS using Cr(VI) as the oxidizer has also been reported and gives much smaller values than the Angus and Glasser method.[19]

XAFS spectra were acquired at the Stanford Synchrotron Radiation Laboratory (SSRL) at Beamline 4-1 using a Si(220) double crystal monochromator detuned 50% to reduce the higher order harmonic content of the beam. All ^{99}Tc samples were triply contained. X-ray absorption spectra were obtained in fluorescence yield mode using a multi-pixel Ge-detector system.[26] In all cases, the grout samples were oriented at 45° relative to both the photon beam and the fluorescence detector. The cuvettes were positioned horizontally as illustrated in Figure 1. The spectra were energy calibrated using the first inflection point of the Tc K-edge spectrum of TcO_4^- adsorbed on Reillex-HPQ™ anion exchange resin defined as 21044 eV.

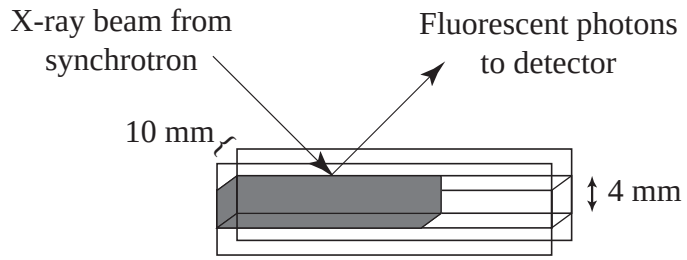

Figure 1: Geometry of a grout sample in semi-micro cuvette used in XAFS experiments.

Extended X-ray absorption fine structure (EXAFS) data analysis was performed by standard procedures[27] using the programs ifeffit,[28] and Athena/Artemis;[29] theoretical EXAFS phases and amplitudes were calculated using FEFF7[30]. All fitting was performed in R-space (R range: 1 to 4.5 Å; k range: 2 to 13.3 $Å^{-1}$; 27 independent points[31]) on k^3 weighted data. Kaiser-Bessel windows were applied to both the R-space and k-space data, with widths of 0.1 Å and 1 $Å^{-1}$, respectively. The EXAFS data for these samples were analyzed with three different models. Model one had only two shells of

neighboring atoms: ~7 S neighbors at 2.38 Å and ~2 Tc neighbors at 2.77 Å. Model two had an additional shell of 6-11 S neighbors with a large static disorder at 4.5 Å. Model three was similar to the second model with an additional Tc neighbor at either 3.8 Å (~1/3 occupancy) or 4.3 Å (~2/3 occupancy). The model chosen as most appropriate was the one whose fit gave the lowest reduced chi-squared, χ^2/ν, where ν is the number of degrees of freedom of the fit: 20, 17, and 13 for models one, two, and three, respectively. For samples 2, 3, and 4, the best model was model three, and for sample 1, model two was slightly better than model three. In addition, all four data sets were fit simultaneously to a single set of parameters for a given model. In this case, the numbers of degrees of freedom were 101, 98, and 94 for models one, two, and three, respectively, and model three gave the best fit.

The X-ray absorption near edge structure (XANES) spectra of the samples were fit using a linear combination the XANES spectra of TcS_x, TcO_4^-, and $TcO_2 \bullet 2H_2O$ as standards, and only the energy calibration of the samples were allowed to vary. This procedure required the careful energy calibration of the XANES spectra of the standards. The fitting was done using the code "fites" developed by C. H. Booth.[32] The fit used 4 parameters (amplitudes of each standard and the energy shift of the sample spectrum), and the XANES spectra had 19 independent data points (150 eV spectra with 8 eV spectral resolution due to a combination of core hole lifetime and instrumental resolution).

The X-ray absorption coefficients for Sample A were determined using Eq 1 where ρ is the sample density (1.7 g cm^{-3}),[19] w_i is the wt. % of element i in the sample, and μ_I is the absorption coefficient of element i (in cm^2 g^{-1}).[33,34] The elemental composition of sample A was determined from the fraction of waste solution, BFS, fly ash, and Portland cement used to prepare the sample, and the elemental compositions of BFS, fly ash, and Portland cement reported by Serne, et al. were used.[5] The X-ray absorption coefficients of sample A at the incident and fluorescent photon energies, $\mu_{tot}(E)$ and $\mu_{tot}(E_f)$, are 5.2 cm^{-1} and 7.5 cm^{-1}, respectively.

$$\mu_{tot} = \rho \sum w_i \mu_i \qquad (1)$$

Results and Discussion

EXAFS studies of initial technetium speciation. A prerequisite for investigating the long-term behavior of technetium in grout is identifying which technetium species are present. While it is obvious that TcO_4^- will be present under oxidizing conditions,[35] the species present under reducing conditions are less obvious. The hydrous Tc(IV) oxide, $TcO_2 \cdot 2H_2O$, results from the reduction of TcO_4^- in the absence of other ligands both in solution and in grout samples.[15,36] In addition, sulfide, either BFS or added to the grout as Na_2S, reduces TcO_4^- to a lower-valent technetium sulfide species thought to be similar to TcS_2.[15] Interestingly, the reaction of sulfide with TcO_4^- in alkaline solution is a known route to Tc_2S_7,[37] which is generally believed to be the technetium species present in reducing CWFs.[16,37] While these results appear to be contradictory, the inconsistency is largely due to the Tc(VII) oxidation state implied by the stoichiometry of Tc_2S_7. If Tc_2S_7 is not actually a Tc(VII) sulfide complex but a lower-valent disulfide complex, no contradiction exists between these previous studies. Although Tc_2S_7 is generally assumed to be a Tc(VII) compound, this assumption has never been examined.[14]

To identify the technetium sulfide species present in reducing grouts, the Tc K-edge EXAFS spectra of the permeable samples were examined shortly after they were prepared. Only these samples contained a single technetium species. All other samples, including these samples at later times, contained more than one species. The permeable samples initially had identical Tc K-edge EXAFS spectra, as shown in Figure 2. The parameters derived by fitting the spectra are listed in Table 2. Therefore, in addition to containing only one technetium species, all of these samples contain the same technetium species, which will be referred to as TcS_x.

Table 2: Initial technetium coordination environment in the permeable samples[a]

Scattering Atom		Sample				
		1[b]	2	3	4	All data[c]
S	N[d]	7.3(5)	7.6(6)	7.0(5)	7.4(6)	7.4(2)
	R(Å)[e]	2.379(5)	2.376(6)	2.381(5)	2.380(5)	2.378(2)
	σ^2(Å^2)[f]	0.0111(7)	0.0118(9)	0.0113(7)	0.0121(8)	0.0117(3)
Tc	N[d]	1.9(4)	1.8(5)	1.6(4)	1.7(4)	1.8(2)
	R(Å)[e]	2.771(4)	2.771(5)	2.779(5)	2.776(5)	2.774(2)
	σ^2(Å^2)[f]	0.007(1)	0.007(1)	0.007(1)	0.007(1)	0.0071(5)
Tc	N[d]	0.3[g]	0.4[g]	0.3[g]	0.3[g]	0.4[g]
	R(Å)[e]	3.80(4)	3.83(3)	3.83(3)	3.86(3)	3.84(1)
	σ^2(Å^2)[f]	0.007[g]	0.005[g]	0.004[g]	0.004[g]	0.006[g]
Tc	N[d]	0.7(2)	0.6(2)	0.7(2)	0.7(1)	0.6(1)
	R(Å)[e]	4.30(3)	4.28(2)	4.29(2)	4.30(3)	4.30(1)
	σ^2(Å^2)[f]	0.006(2)	0.005(2)	0.004(1)	0.004(2)	0.006(1)
S	N[d]	11(11)	6(6)	6(6)	6(5)	5(2)
	R(Å)[e]	4.48(3)	4.47(3)	4.48(3)	4.49(3)	4.47(1)
	σ^2(Å^2)[f]	0.02(1)	0.02(1)	0.01(1)	0.01(1)	0.012(4)
	ΔE_0	0.4(7)	0.8(8)	0.6(7)	0.5(8)	0.7(3)
	R[h]	0.078	0.096	0.082	0.085	0.102

a) The number in parentheses is the standard deviation of the parameter obtained by fitting the EXAFS data. In comparison to crystallographic data, N differs by up to 25%, and in R by 0.5%.

b) The best model for the EXAFS spectrum of sample 1 did not include the Tc shells at 3.82 and 4.31 Å, but this model is included for comparison with the other samples.

c) All data fit simultaneously using a single set of parameters.

d) N: number of neighboring atoms.

e) R: distance from the scattering atom to the technetium center.

f) σ^2: Debye-Waller parameter, the amount of disorder in the distance to the neighboring atoms.

g) Parameter determined from the corresponding parameter in the following shell.

h) $\text{R-factor} = \left(\sum(y_i(\text{data}) - y_i(\text{fit}))^2 / \sum(y_i(\text{data}))^2\right)^{1/2}$.

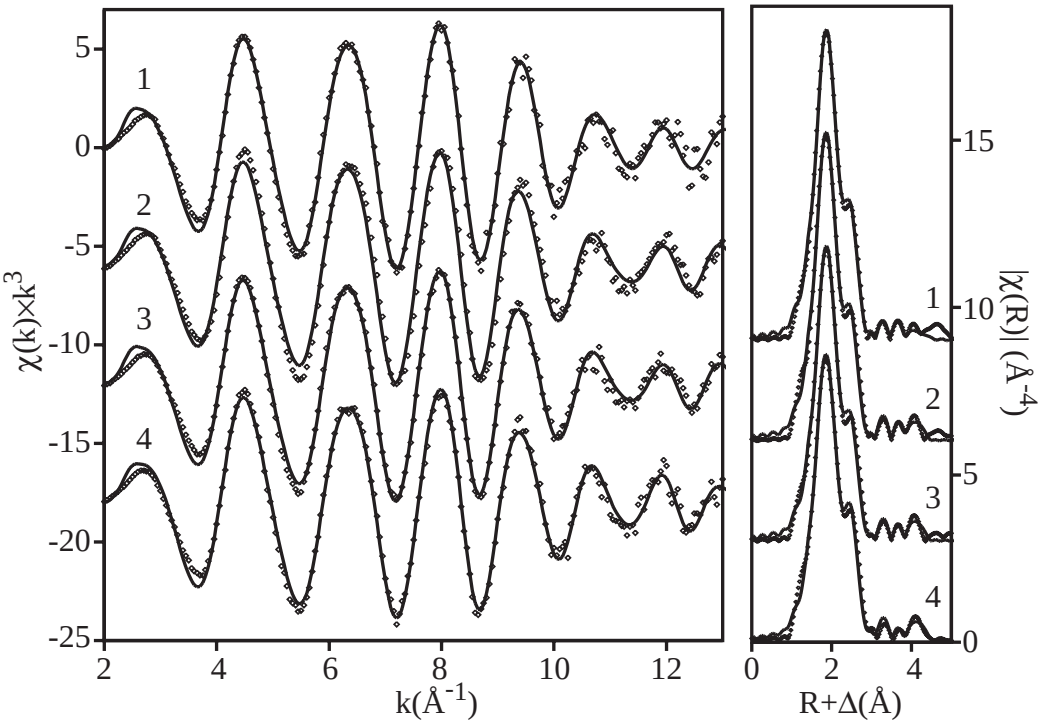

Figure 2: Tc K-edge EXAFS spectra (left) and their Fourier transforms (right) of the technetium species initially present in grout samples prepared by reducing the TcO_4^- with excess sodium sulfide. Data is shown as dots and the fits are shown as lines (Fit range: k = 2 to 13.3 $Å^{-1}$; R = 1 to 4.5 Å). Sample numbers are indicated next to the traces.

The coordination environment of TcS_x can be described by considering the first two and last three coordination shells separately. The first two coordination shells, which comprise the largest features in the Fourier transforms, consist of ~7 sulfur neighbors at 2.37 Å and 2 technetium nearest neighbors at 2.77 Å. These distances and coordination numbers are similar to those of the molybdenum sulfide complex, $Mo_3(\mu^3\text{-}S)(S_2)_6^{2-}$, shown in Figure 3, in which each molybdenum center has 7 sulfur and 2 molybdenum neighbors at 2.44 and 2.72 Å, respectively.[38] The $Mo_3(\mu^3\text{-}S)(\mu\text{-}S_2)_3$ core of this complex, without the triply bridging sulfide, forms the building block of the MoS_3 structure,[39] which has an EXAFS spectrum similar to that of TcS_x.[40,41] The nearest neighbor environments in both compounds are analogous; in MoS_3, each molybdenum center has ~6 sulfur neighbors at 2.44 Å and 2 molybdenum neighbors at 2.75 Å. The similarities of the distances and coordination numbers of the first two

coordination shells of MoS_3, $Mo_3S(S_2)_6^{2-}$ and TcS_x strongly suggest that the TcS_x structure contains the same triangular core, $Tc_3(\mu^3\text{-}S)(\mu\text{-}S_2)_3S_6$ as shown in Figure 3. Furthermore, the 2.77 Å Tc-Tc distance is typical for such a triangular complex composed of seven-coordinate metal centers; analogous triangular complexes with six-coordinate metal centers have substantially shorter metal-metal distances.[42]

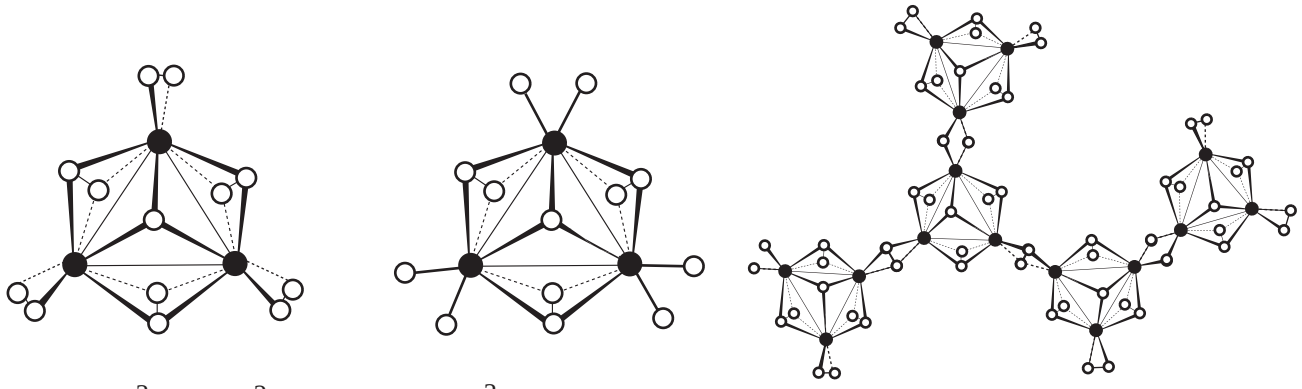

Figure 3: Structures of $Mo_3(\mu^3\text{-}S)(S_2)_6^{2-}$, the proposed structure of the analogous $Tc_3(\mu^3\text{-}S)(S_2)_3S_6$ core that forms the building block of TcS_x, and the proposed structure of TcS_x (only a portion of the extended structure is illustrated). Metal atoms are illustrated by solid circles, sulfur atoms are depicted by open circles.

The last three coordination shells give rise to the small features at higher R in the Fourier Transform. The uncertainty in the assignments of these last shells is much greater than for the first two shells except for the additional sulfur atoms at 4.5 Å, which much be present in the $Tc_3(\mu^3\text{-}S)(S_2)_3S_6$ core. In addition to the additional sulfur atoms, each technetium has a next-nearest technetium neighbor at either 3.8 Å (~1/3 of the technetium centers) or 4.3 Å (~2/3 of the technetium centers). The two different Tc-Tc distances suggest that different ligands bridge the technetium centers. Since the presence of 7 first shell sulfur neighbors requires that each technetium center has two sulfur atoms capable of bridging adjacent technetium centers, possible identities of the bridging ligands are two bridging sulfide (or hydrosulfide) ligands or an edge-bound disulfide similar to the bridging disulfide of the $Tc_3(\mu^3\text{-}S)(\mu\text{-}S_2)_3$ cluster

without the Tc-Tc bond. The Tc-Tc distance of two technetium centers symmetrically bridged by an edge-bound disulfide ligand would be close to 4.3 Å. In a similar copper complex,[43] two Cu centers are separated by 4.03 Å, but the Tc-S bonds in TcS_x are 0.1 Å longer than the Cu-S bonds. Moreover, the S-S distance of the disulfide bridge, determined from the Tc-Tc and Tc-S distances, must be 2.0 Å, typical for a bridging disulfide.[38,43] For these reasons, the 4.3 Å Tc-Tc distance is assigned to two Tc centers symmetrically bridged by a disulfide ligand.

The 3.8 Å Tc-Tc distance could be due to either two bridging sulfide or hydrosulfide ligands. If the Tc and S atoms are coplanar, the Tc-Tc and Tc-S distances produce a Tc-S-Tc angle of 109°. Although few families of complexes exist in which the parameters for bridging sulfide and hydrosulfide ligands can be compared directly, a M-S-M angle of 109° is more typical of a bridging sulfide than of a hydrosulfide, which generally have M-(SH)-M angles of ~100°.[44-46] For this reason, the 3.8 Å Tc-Tc distance is assigned to two Tc centers symmetrically bridged by two sulfide ligands. Overall, the EXAFS data is consistent with a TcS_x structure composed of triangular $Tc_3(\mu^3\text{-}S)(\mu\text{-}S_2)_3$ clusters linked by either bridging disulfide or by two bridging sulfide ligands as shown in Figure 3.

Although the assignments of the last two technetium scattering shells in the EXAFS spectrum of TcS_x is much less certain than the assignments of the other three shells, the resulting model provides the best fit to the data as judged by the reduced χ^2 value. In addition, the resulting bond distances can be interpreted in a chemically meaningful and reasonable manner. For these reasons, the model that best describes the EXAFS spectrum of TcS_x is the one given in Table 2 and shown in Figure 3.

The structure of TcS_x has a stoichiometry of $Tc_3S_2(S_2)_4$ or Tc_3S_{10}, which is almost identical to the stoichiometry of $TcS_{3.2}$ determined for "Tc_2S_7" prepared under similar conditions.[37] Since the conditions used to prepare grout samples are analogous to those used to prepare Tc_2S_7, it seems likely

that TcS_x and Tc_2S_7 are the same compound. However, the technetium centers in TcS_x are clearly not heptavalent. From the EXAFS model, TcS_x would be a Tc(IV) compound, which is consistent with its Tc-K edge absorption energy, 6.5 eV below that of TcO_4^-. For comparison, the energies of the Tc-K edges of Tc(IV) complexes with oxygen coordination shells occur at ~5.5 eV below that of TcO_4^-.[17] Consequently, the technetium sulfide species present in reducing containing grouts, TcS_x, appears to be Tc_2S_7 as previously suggested;[16,37] however, the technetium centers in TcS_x are most likely tetravalent in agreement with the previous XAFS study.[15]

Evolution of technetium speciation determined by XANES spectroscopy. The speciation of technetium in the grout samples was determined by least squares fitting of the XANES spectra using the XANES spectra of $TcO_2 \cdot 2H_2O$, TcO_4^-, and TcS_x as components. This method is analogous to those previously described by Ressler et al. and Panak et al., which have been shown to yield quantitative speciation information assuming that appropriate, correctly calibrated standards are employed.[47,48] The results for the evolution of technetium speciation in the permeable and impermeable samples is addressed separately.

Permeable samples. As described in the previous section, the technetium speciation of all the permeable samples was initially identical since all samples contained only TcS_x. However, as the samples aged, their XANES spectra changed as shown in Figure 4, which also shows the deconvolution of the XANES spectrum of a 45-month-old sample. The mole fraction of TcO_4^- in these samples is shown in Figure 5 as a function of the age of the sample. The scatter of the data shown in Figure 5 is much greater than the standard deviation of the measurement and will be discussed below. Unfortunately, this large degree of scatter results in a correspondingly large uncertainty in the rate of oxidation of Tc(IV) in these samples. However, Figure 5 shows that NO_3^- does not play a major role in the oxidation of Tc(IV) in these samples since the degree of oxidation of all samples is approximately equivalent despite the fact that samples 2 and 4 do not contain NO_3^-.

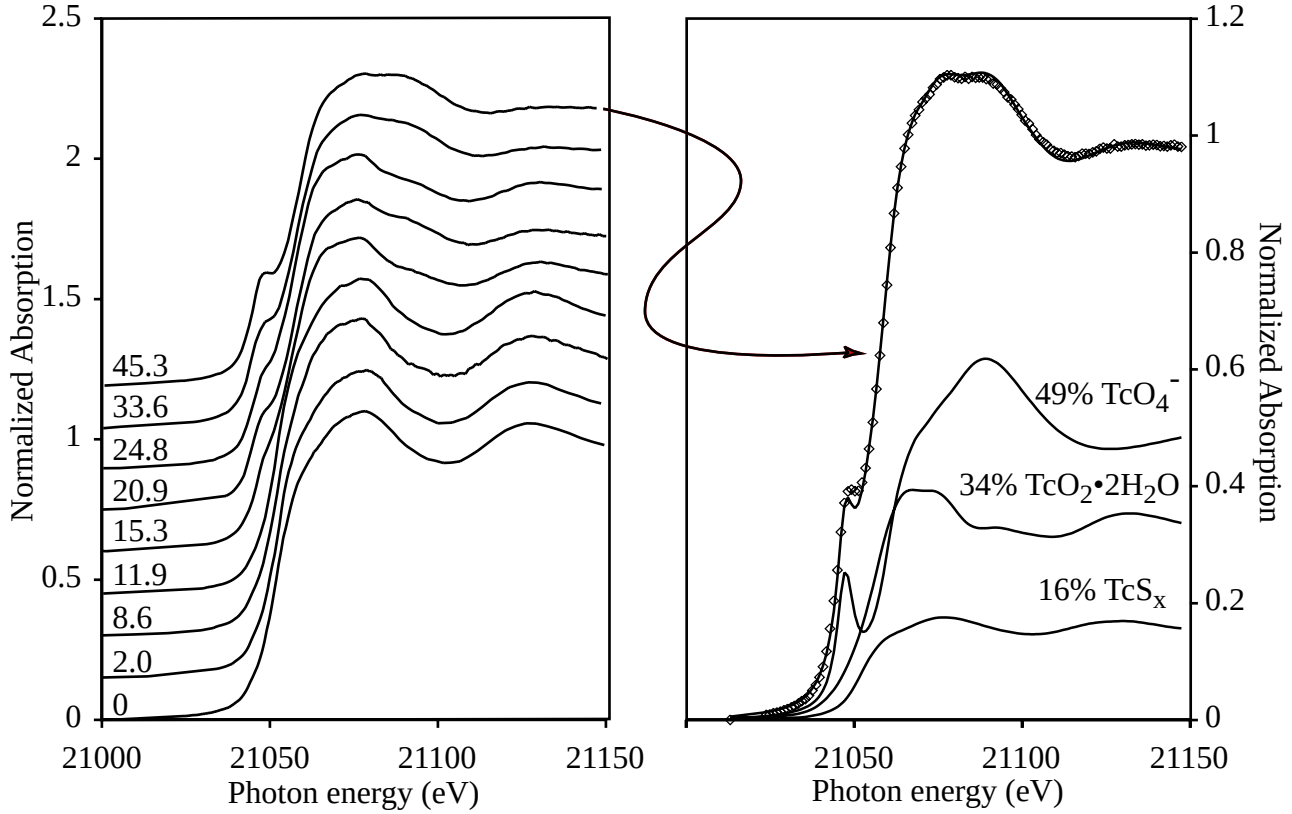

Figure 4: (left) Evolution of the Tc-K edge XANES spectra of sample 4 as a function of age. The age of cement (in months) is given next to the corresponding spectrum. (right) Deconvolution of the XANES spectrum of a 45 month old sample. Data are shown as dots and the least squares fit is shown as a line.

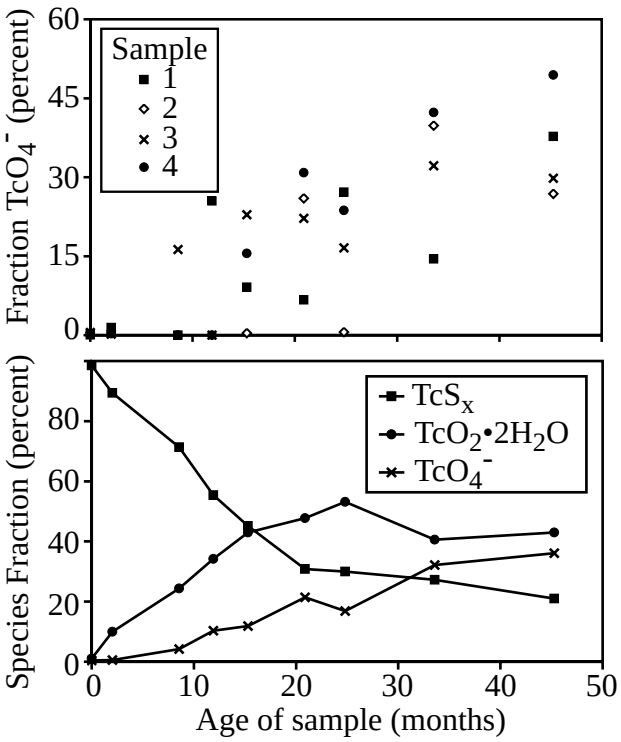

Figure 5: (upper) Evolution of the fraction of technetium present as TcO_4^- in the permeable samples as a function of age. (lower) Evolution of technetium speciation in the permeable samples averaged over all samples.

Permeable samples. In contrast to the permeable samples, ~20% of the TcO_4^- in the impermeable samples was not reduced to Tc(IV) at the beginning of the experiment. However, as the samples aged, the amount of TcO_4^- decreased, as shown in Figure 6, presumably from its reaction with the BFS in the grout.[15] The large increase in the amount of TcO_4^- observed in samples A and C at 26 months is due to exposure of these samples to atmosphere; sample B remained sealed. Based on the assumption that the fraction of TcO_4^- in these samples is the same at 26 months as when it was previously determined at 18 months, the fraction of TcO_4^- present in Samples A and C increased by 34% and 46%, respectively, during the 4 months that they were exposed to air. In comparison to the permeable samples, less scatter is present in the fraction of TcO_4^- in these samples and the fraction of TcO_4^- varies little among the samples until samples A and C were exposed to air. As in the permeable samples, the presence of NO_3^- has no observable effect on the speciation of technetium.

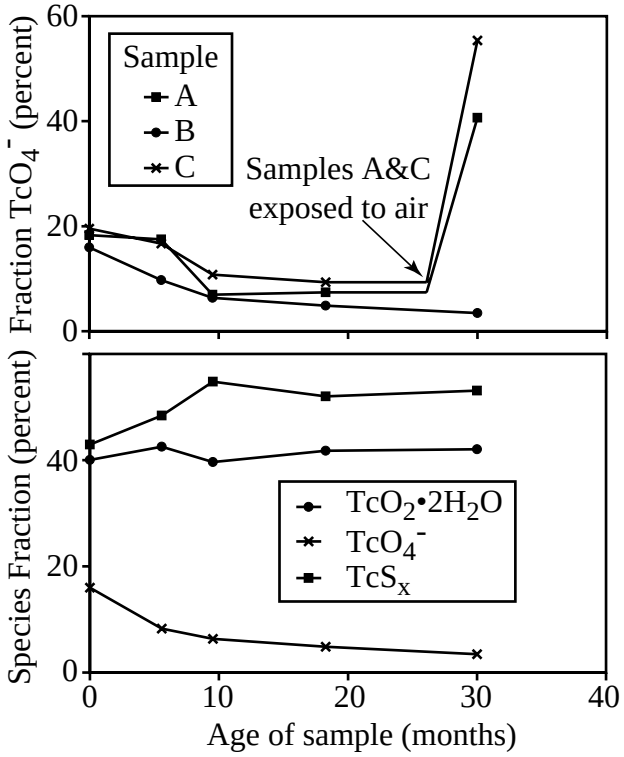

Figure 6: (upper) Evolution of the fraction of technetium present as TcO_4^- in the impermeable samples as a function of age. Arrow indicates that samples A and C were opened at 26 months (the fraction TcO_4^- at that point is assumed to be the same as previously determined at 18 months). (lower) Evolution of technetium speciation in sample B, which remained sealed throughout the experiment.

Discussion

The data from both series of samples show that TcS_x in grout is unstable towards oxidation. As noted previously, both NO_3^- and O_2 could oxidize the lower-valent technetium species present in these samples. Since the presence of NO_3^- had no significant effect on the rate of oxidation of technetium in these samples, atmospheric O_2 is the likely oxidizing agent. In addition, oxidation by O_2 rather than by NO_3^- helps explain the scatter in the speciation data observed in the permeable samples.

The scatter in the data in Figure 5 is believed to result from a variation in the amount of O_2 diffusing into the samples, which produces different amounts of oxidized TcS_x in different areas of the samples. Since the regions probed by the X-ray beam were chosen arbitrarily, such spatial inhomogeneity of the Tc speciation would result in the sort of scatter observed in Figure 5. Although the O_2 diffusion into the samples was originally thought to result from air leaking through the caps of the PS cuvettes, XANES spectra obtained at intervals from the top of the samples to the bottom show that this is not the case; instead, the technetium speciation varies somewhat along the length of the cuvette (Figure 7). Interestingly, O_2 is diffusing into the impermeable samples through the ~1 cm thick epoxy plug, but not through the ~2 mm thick PMMA cuvette, as indicated by the presence of TcO_4^- at the top of the cuvette (Figure 7). In the case of the permeable samples, the variation in the rate of O_2 diffusion is believed to be caused by the ridged walls of the cuvette through which the XAFS spectra were obtained since O_2 would diffuse more quickly through the thinner areas between the ridges.

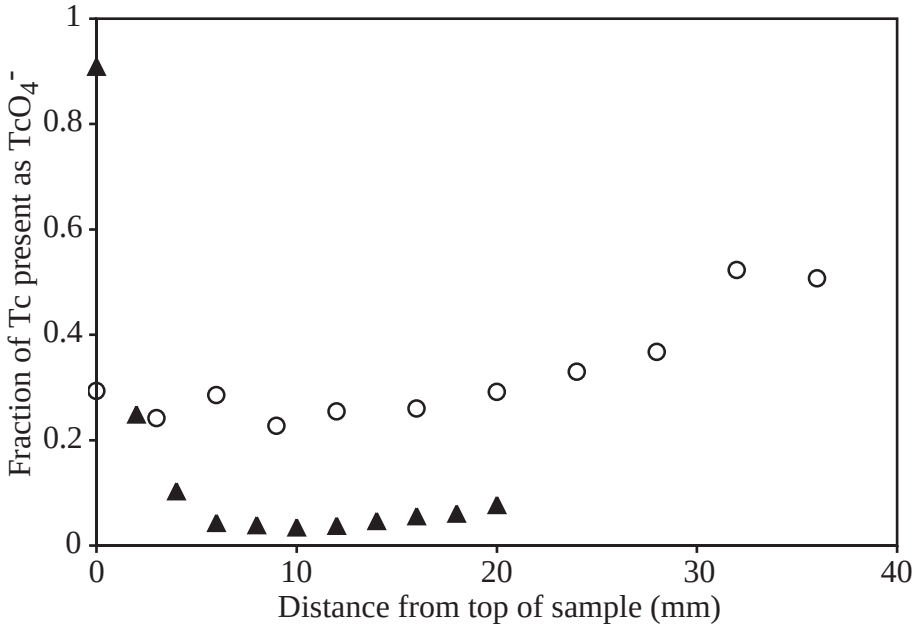

Figure 7: Technetium speciation as a function of position within permeable sample 1 (circles) and impermeable sample B (triangles). Age of sample 1, 73 months; sample B, 59 months.

The premise that O_2 is the actual oxidizer is strongly supported by the results from the impermeable

samples shown in Figure 6. Although ~20% of the TcO_4^- in these samples was not reduced to TcS_x, the amount of TcO_4^- in these samples declined at later times, presumably due to reduction by BFS. Furthermore, the technetium speciation in the impermeable samples is relatively homogeneous (except near the top). Although the technetium speciation evolved and the portions of the samples probed by XANES were arbitrarily chosen, little scatter exists in the technetium speciation among the different samples. Since, atmospheric O_2 cannot readily diffuse into these samples, technetium speciation should not vary with position. However, the most dramatic evidence for O_2 oxidation is the 40% increase in the amount of TcO_4^- observed in the initially sealed impermeable samples after 4 months exposure to atmosphere.

One unexpected result is the appearance of $TcO_2•2H_2O$ in the permeable samples as they aged. Formation of $TcO_2•2H_2O$ cannot result from the hydrolysis of TcS_x since it is stable to hydrolysis under the conditions present in the grout samples. Rather, the observation of $TcO_2•2H_2O$ implies that the oxidation of TcS_x proceeds by initial oxidation to $TcO_2•2H_2O$, which is then oxidized to TcO_4^- as shown in Eqs 2 and 3. This hypothesis is also supported by the evolution of the technetium speciation shown in the lower panel of Figure 5. Initial oxidation of TcS_x to $TcO_2•2H_2O$ is consistent with the potentials for the reduction of SO_4^{2-} to S^{2-} (-0.67 V) and of TcO_4^- to $TcO_2•2H_2O$ (-0.28 V) at pH 13. Although the detailed mechanism is certainly more complex than this simple picture, the observation of $TcO_2•2H_2O$ in the permeable samples is consistent with the premise that oxidation of TcS_x to TcO_4^- proceeds with $TcO_2•2H_2O$ as an intermediate.

$$Tc_3S_{10} + 18\ O_2 + 20\ HO^- \rightarrow 3\ TcO_2•2H_2O + 10\ SO_4^{2-} + 4\ H_2O \qquad (2)$$

$$4\ TcO_2•2H_2O + 4\ HO^- + 3\ O_2 \rightarrow 4\ TcO_4^- + 10\ H_2O \qquad (3)$$

The oxidation of the impermeable samples that have been removed from their cuvettes should occur at all of surfaces of the grout sample as illustrated in Figure 8. Consequently, the XAFS experiment examines a layer of oxidized grout on the surface of a sample consisting mainly of reduced grout, based on the reasonable assumption that oxidation of reducing grout proceeds by the shrinking core mechanism as proposed by Smith and Walton.[16] The thickness of the oxidized region formed in the initially sealed samples after exposure to atmosphere can be determined from the fraction of technetium that is oxidized using the formula for the fluorescence yield from a sample of a given thickness.[49,50] For a sample of thickness d, the fluorescence yield is given by Eq 4, where A is the area of the detector, r is the distance from the sample to the detector, ε_{Tc} is the fluorescence yield from the technetium K-shell, μ_{Tc} is the technetium absorption coefficient at the incident photon energy, $\mu_{tot}(E)$ and $\mu_{tot}(E_f)$ are the total absorption coefficients of the sample at the incident and fluorescent photon energies, and θ, ϕ, and d are defined in Figure 8. Since the total fluorescence yield for a thick sample is given by Eq 5, the contribution of a surface layer of thickness, d, to the total fluorescence signal is given by Eq 6, where I_d is the fluorescence from a surface layer of thickness, d, and I_{tot} is the total fluorescence from the sample. For the impermeable samples exposed to air, the average increase in pertechnetate content of 40 %, or I_d/I_{tot}=0.4 in Eq 5, corresponds to a 0.28 mm thick oxidized layer, using $\mu_{tot}(E)$ and $\mu_{tot}(E_F)$ calculated for sample A. Because 99% of the fluorescence from this sample comes from the upper 2.6 mm of the 4 mm thick sample, the sample can be considered thick and the contribution to the fluorescence of the oxidized layer on the opposite side of the sample can be ignored.

$$I_d/I_0(E) \propto \frac{A}{r^2}\varepsilon_{Tc}\frac{\mu_{Tc}(E)}{\mu_{tot}(E)+\mu_{tot}(E_f)\frac{\sin\phi}{\sin\theta}}\left\{1-\exp\left[-\left(\frac{\mu_{tot}(E)}{\sin\phi}+\frac{\mu_{tot}(E_f)}{\sin\theta}\right)d\right]\right\} \qquad (4)$$

$$I_{tot}/I_0(E) \propto \frac{A}{r^2}\varepsilon_{Tc}\frac{\mu_{Tc}(E)}{\mu_{tot}(E)+\mu_{tot}(E_f)\frac{\sin\phi}{\sin\theta}} \qquad (5)$$

$$\frac{I_d}{I_{tot}} = 1 - \exp\left[-\left(\frac{\mu_{tot}(E)}{\sin\phi} + \frac{\mu_{tot}(E_f)}{\sin\theta}\right)d\right] \qquad (6)$$

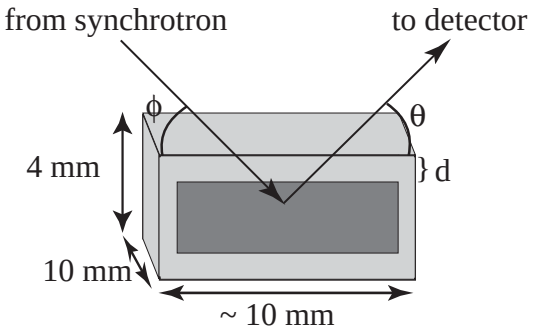

Figure 8: Illustration of the XAFS experiment on an initially sealed, impermeable sample that has been exposed to air. The oxidized layer of thickness d is illustrated by the lighter colored region and is on the surface of the darker colored reducing grout.

The thickness of the oxidized layer calculated from the fraction of TcO_4^- present in the sample can be compared with the thickness of the oxidized region determined analogously using the shrinking core model of Smith and Walton.[16] The difference between the model employed here and the Smith and Walton model is that here the effective diffusion coefficient of oxygen, $D_{eff(O2)}$, is determined from the MacMullin number and the diffusion coefficient of oxygen in water: $D_{eff(O2)} = D_{m(O2)}/N_m$ as described earlier. The rate of growth of the oxidized layer of thickness d is given by Eq 7 where t is time (in seconds), C_{O2} is the concentration of oxygen in water at the surface of the grout (3.7×10^{-7} mol cm^{-3}), $D_{m(O2)}$ is the diffusion coefficient of oxygen in water (2.0×10^{-5} cm^2 s^{-1}), and C_{red} is the concentration of reducing equivalents in the CWF in moles of electrons (3.7×10^{-4} mol cm^{-3} for a CWF with a density of 1.7 g cm^{-3} composed of 27% BFS with a measured reducing capacity of 0.81 meq g^{-1}, all other grout

components are assumed to have a negligible reducing capacity). Using Eq 7, the thickness of the oxidized region determined from the XANES experiment, 0.28 mm, in grout samples exposed to air for 120 days corresponds to a N_m of 1.6×10^3 or a $D_{eff(NO3-)}$ of 9.5×10^{-9} cm^2 s^{-1}, which is within the range of $D_{eff(NO3-)}$ reported for CWFs. The thickness of the oxidized layer determined from the XANES experiment is consistent with the thickness of the oxidized layer anticipated from the shrinking core model of Smith and Walton.

$$d = \sqrt{\frac{8C_{O_2}tD_{m(O_2)}}{N_m C_{red}}} \qquad (7)$$

The effect of oxidation by O_2 on an actual waste form, Saltstone, also can be examined using this model to illustrate the difference between oxidation of reduced technetium species by O_2 and NO_3^-. In comparison to sample A, Saltstone has smaller $D_{eff(NO3-)}$, ranging from 1.3×10^{-9} cm^2 s^{-1} to 5×10^{-9} cm^2 s^{-1}, but a similar C_{red} since Saltstone is prepared from the same BFS in similar proportions to those used to prepare Sample A. Using a $D_{eff(NO3-)}$ of 5×10^{-9} cm^2 s^{-1}, the thickness of the oxidized region would be 17 cm after one ^{99}Tc half-life (213,000 yr), and after ten half-lives, the oxidized region would be 53 cm thick. For comparison, the dimensions of a Savannah River Saltstone monolith are 30.5 m × 30.5 m × 7.5 m.[7] Therefore, approximately 6% of the technetium in the waste form would be oxidized after one ^{99}Tc half-life, and approximately 20% would be oxidized after ten half-lives based on the assumption that oxidation occurs at all sides of the Saltstone cell. This simple estimate ignores the presence of concrete vault surrounding the Saltstone and the layer of reducing grout without technetium at the top of the Saltstone vault, both of which would decrease the rate of ^{99}Tc leaching. Cracking and flow of surface water through the CWF could greatly increase the rate of oxidation and the leaching of TcO_4^- by effectively decreasing the size of the Saltstone cell to the intercrack spacing,[7,8] so this discussion is intended only to illustrate the difference between oxidation by O_2, which produces an oxidized surface region with an increased $D_{eff(99Tc)}$, and oxidation by NO_3^-, which would result in an increased

$D_{eff(99Tc)}$ throughout the entire volume of the waste. The results in this study indicate that the oxidation of Tc(IV) species in these grout samples is due solely to O_2, and that NO_3^- has no observable effect on the speciation of technetium in these samples. While these results do not show that NO_3^- is unreactive towards Tc(IV) in reducing grouts, this reaction occurs too slowly to be observed in this study.

ACKNOWLEDGMENT. The authors thank Corwin Booth for helpful discussions about least squares fitting of the XANES and EXAFS data and for the use of the code "fites". The authors thank Christine Langton for providing the pulverized fly ash, BFS, and Portland cement. This work was supported by the Environmental Management Science Program of the U.S. DOE Office of Science, Biological and Environmental Research, Environmental Remediation Sciences Division and was performed at the Lawrence Berkeley National Laboratory, which is operated by the U. S. DOE under Contract No. DE-AC03-76SF00098. Portions of this research were carried out at the Stanford Synchrotron Radiation Laboratory, a national user facility operated by Stanford University on behalf of the U.S. Department of Energy, Office of Basic Energy Sciences.

SUPPORTING INFORMATION AVAILABLE: Detailed description of EXAFS model selection criteria; composition of Sample A used to determine the X-ray absorption coefficients; Tables of the data shown in Fig. 5 and 6; plots of the evolution of the XANES spectra of Sample B and an example of a XANES fit for Sample B; derivation of the shrinking core model used to obtain Eq 7. This information is available free of charge via the Internet at http://pubs.acs.org.

REFERENCES

(1) Gray, R. H.; Becker, C. D. *Environ. Manage.* **1993**, *17*, 461.
(2) "Response to Requirement for Report to Congress Under Floyd D. Spence National Defense Authorization Act for Fiscal Year 2001," Office of River Protection, 2000.
(3) Oblath, S. B. "Relative Release Rates of Nitrate, Tc, Cs, and Sr from Saltstone," DPST-84-620, Savannah River Laboratory, 1984.
(4) Oblath, S. B. *Environ. Sci. Technol.* **1989**, *23*, 1098.
(5) Serne, R. J.; Lokken, R. O.; Criscenti, L. J. *Waste Manage.* **1992**, *12*, 271.

(6) National Research Council. *Research Needs for High-Level Waste Stored in Tanks and Bins at U.S. Department of Energy Sites*; National Academy Press: Washington, D.C., 2001.
(7) Seitz, R. R.; Walton, J. C.; Dicke, C. A.; Cook, J. R. *Mat. Res. Soc. Symp. Proc.* **1993**, *294*, 731.
(8) Kaplan, D. I.; Serne, R. J. *Radiochim. Acta* **1998**, *81*, 117.
(9) Gilliam, T. M.; Spence, R. D.; Bostick, W. D.; Shoemaker, J. L. *J. Hazard. Mater.* **1990**, *24*, 189.
(10) MacMullin, R.; Muccini, G. *Am. Inst. of Chem. Engin., J.* **1956**, *2*, 393.
(11) Taffinder, G. G.; Batchelor, B. *J. Environ. Eng.* **1993**, *119*, 17.
(12) Langton, C. A. "Challenging Applications for Hydrated and Chemically Reacted Ceramics," DP-MS--88-163, Savannah River Laboratory, 1988.
(13) Yeh, B. S.; Wills, G. B. *J. Chem. Engin. Data* **1970**, *15*, 187.
(14) Rard, J. A.; Rand, M. H.; Anderegg, G.; Wanner, H. *Chemical Thermodynamics of Technetium*; Elsevier Science: Amsterdam, 1999.
(15) Allen, P. G.; Siemering, G. S.; Shuh, D. K.; Bucher, J. J.; Edelstein, N. M.; Langton, C. A.; Clark, S. B.; Reich, T.; Denecke, M. A. *Radiochim. Acta* **1997**, *76*, 77.
(16) Smith, R. W.; Walton, J. C. *Mat. Res. Soc. Symp. Proc.* **1993**, *294*, 247.
(17) Lukens, W. W.; Bucher, J. J.; Edelstein, N. M.; Shuh, D. K. *Environ. Sci. Technol.* **2002**, *36*, 1124.
(18) Bajt, S.; Clark, S. B.; Sutton, S. R.; Rivers, M. L.; Smith, J. V. *Anal. Chem.* **1993**, *65*, 1800.
(19) Kaplan, D. I. "Estimated Duration of the Subsurface Reducing Environment Produced by the Z-Area Saltstone Disposal Facility (U)," WSRC-RP-2003-00362, Westinghouse Savannah River Company, 2003.
(20) Kneas, K. A.; Demas, J. N.; Nguyen, B.; Lockhart, A.; Xu, W.; DeGraff, B. A. *Anal. Chem.* **2002**, *74*, 1111.
(21) Gao, Y.; Ogilby, P. R. *Macromolecules* **1992**, *25*, 4962.
(22) Hormats, E. I.; Unterleitner, F. C. *J. Phys. Chem.* **1965**, *69*, 3677.
(23) Angus, M. J.; Glasser, F. P. *Mat. Res. Soc. Symp. Proc.* **1985**, *50*, 547.
(24) Walden, G. H.; Hammett, L. P.; Chapman, R. P. *J. Am. Chem. Soc.* **1931**, *53*, 3908.
(25) Smeller, J. A. *Amer. Lab. News* **1999**, *October*, 6.
(26) Bucher, J. J.; Allen, P. G.; Edelstein, N. M.; Shuh, D. K.; Madden, N. W.; Cork, C.; Luke, P.; Pehl, D.; Malone, D. *Rev. Sci. Instrum.* **1996**, *67*, 4.
(27) Koningsberger, D. C.; Prins, R. *X-Ray Absorption: Principles, Applications, Techniques of EXAFS, SEXAFS, and XANES*; John Wiley & Sons: New York, 1988.
(28) Newville, M. *J. Synchrotron Rad.* **2001**, *8*, 322.
(29) Ravel, B. *Physica Scripta* **2003**, *in press*.
(30) Rehr, J. J.; Albers, R. C.; Zabinsky, S. I. *Phys. Rev. Lett.* **1992**, *69*, 3397.
(31) Stern, E. *Phys. Rev. B* **1993**, *48*, 9825.
(32) Sarrao, J. L.; Immer, C. D.; Fisk, Z.; Booth, C. H.; Figueroa, E.; Lawrence, J. M.; Modler, R.; Cornelius, A. L.; Hundley, M. F.; Kwei, G. H.; Thompson, J. D.; Bridges, F. *Phys. Rev. B* **1999**, *59*, 6855.
(33) McMaster, W.; Kerr Del Grande, N.; Mallett, J.; Hubbell, J. "Compilation of X-ray Cross Sections," UCRL-50174, Lawrence Livermore National Laboratory, 1969.
(34) Bandyopadhyay, B., "Mucal on the web," http://www.csrri.iit.edu/mucal.html.
(35) Colton, R. *The Chemistry of Technetium and Rhenium*; Interscience Publishers: New York, 1965.
(36) Cartledge, G. H. *J. Electrochem. Soc.* **1971**, *118*, 231.
(37) Lee, S. Y.; Bondietti, E. A. *Mat. Res. Soc. Symp. Proc.* **1983**, *15*, 315.
(38) Müller, A.; Pohl, S.; M., D.; Cohen, J. P.; Bennett, J. M.; Kirchner, R. M. *Z. Naturforsh.* **1979**, *34b*, 434.
(39) Weber, T.; Muijsers, J. C.; Niemantsverdriet, J. W. *J. Phys. Chem.* **1995**, *99*, 9194.
(40) Hibble, S. J.; Rice, D. A.; Pickup, D. M.; Beer, M. P. *Inorg. Chem.* **1995**, *34*, 5109.

(41) Cramer, S. P.; Liang, K. S.; Jacobson, A. J.; Chang, C. H.; Chianelli, R. R. *Inorg. Chem.* **1984**, *23*, 1215.
(42) Müller, A.; Jostes, R.; Cotton, F. A. *Angew. Chem. Int. Ed. Engl.* **1980**, *19*, 875.
(43) Fujisawa, K.; Moro-oka, Y.; Kitajima, N. *J. Chem. Soc., Chem. Commun.* **1994**, 623.
(44) Mueting, A. M.; Boyle, P.; Pignolet, L. H. *Inorg. Chem.* **1984**, *23*, 44.
(45) Bianchini, C.; Mealli, C.; Meli, A.; Sabat, M. *Inorg. Chem.* **1986**, *25*, 4617.
(46) Pleus, R. J.; Waden, H.; Saak, W.; Haase, D.; Pohl, S. *J. Chem. Soc., Dalton Trans.* **1999**, 2601.
(47) Ressler, T.; Wong, J.; Roos, J.; Smith, I. L. *Environ. Sci. Technol.* **2000**, *34*, 950.
(48) Panak, P.; Booth, C.; Caulder, D.; Bucher, J.; Shuh, D.; Nitsche, H. *Radiochim. Acta* **2002**, *90*, 315.
(49) Goulon, J.; Goulon-Ginet, C.; Cortes, R.; Dubois, J. M. *J. Physique* **1982**, *43*, 539.
(50) Tröger, L.; Arvanitis, D.; Baberschke, K.; Michaelis, H.; Grimm, U.; Zschech, E. *Phys. Rev. B* **1992**, *46*, 3283.

KEYWORDS technetium, cement, grout, nuclear waste

BRIEF The speciation of technetium in reducing grout samples was examined using X-ray absorption fine structure spectroscopy; the reduced technetium species were oxidized by atmospheric oxygen.